Journal of Materials Chemistry C

RSC Publishing

PAPER

View Article Online
View Journal | View Issue

Cite this: J. Mater. Chem. C, 2013, 1, 5309

A new class of "electro-acid/base"-induced reversible methyl ketone colour switches†

Yu-Mo Zhang,[a] Minjie Li,*[a] Wen Li,[a] Zhiyuan Huang,[a] Shaoyin Zhu,[a] Bing Yang,[a] Xiao-Chun Wang[b] and Sean Xiao-An Zhang*[a]

Received 24th April 2013
Accepted 25th June 2013

DOI: 10.1039/c3tc30769g

www.rsc.org/MaterialsC

Methyl ketone has been designed as a switching unit for electrically addressable molecular colour switches. A newly proposed mechanism of "electro-acid/base" (radical ions)-induced intermolecular proton transfer for the colour switch is proven clearly by cyclic voltammetry (CV), X-ray photoelectron spectroscopy (XPS), infrared spectroscopy (IR) and *in situ* UV-Vis spectroscopy. A dramatic spectral absorption shift (about 291 nm) is observed during the switching, and blue, yellow and green colours are obtained by adjusting the substituents on the methyl ketone-bridged unit. The *in situ* "electro-acid/base" is far more convenient than the conventional chemical stimulus of acids or bases for the manipulation of the molecular switching properties. This new switching method and molecular structure manipulation will inspire and accelerate the further development of broad switching materials and applications in ultrathin flexible displays, *etc.*

Introduction

Electro-switchable organic colour materials have been intensively investigated over the past decades due to their broad applications in displays,[1] data recording,[2] sensing,[3] optical communication,[4] *etc.* Most of the colour switching is based on a mechanism featuring the direct redox state change of the materials, and they can be divided into two main categories. The first class involves conjugated oligomers and polymers,[5] such as polythiophenes,[6] polyaniline[7] and polyselenophene.[8] These materials have the advantage of easy processing, and the disadvantage of slow response times that limits practical applications. The second category includes small organic molecules, such as 2,2′-bipyridine derivatives,[9] 5-substituted isophthalate derivatives[10] and organometallic compounds.[11] These materials have better colour intensity and a faster response time, but usually suffer from instability and poor reversibility and processability. Thus, there has been the constant need for developing better electro-switchable organic colour materials.

We believe it is possible to develop good colour-switchable molecules by constructing multiple aromatic units with quick alternative connection units, and methyl ketone seems a good candidate for such a switchable bridge, as it undergoes a reversible enol–ketone tautomerization on pH changes. The transformation between the keto and enol forms would function as a switchable bridge for alternative extended conjugation. Additionally, both the colour tuning and processability of this class of molecules could be easily improved by varying the substituents on the aromatic rings. Recent research has indicated that the keto–enol tautomerization can be manipulated by photo-acid induced intramolecular proton transfer.[12] This inspires us to investigate the possibility of using electrically generated radical ions as a trigger to induce the keto–enol tautomerization. However, no reports have demonstrated that the equilibrium of the keto–enol tautomerization can be manipulated by an electric field, which is because the keto–enol tautomerization usually needs to be induced by a stronger acid/base, and multiple electrochemical/electrophysical factors make the elucidation of the reaction mechanism extremely intricate.

Herein we report the first example of using radical ions as convenient acids or bases *in situ* for the reversible manipulation of the structure and properties of methyl ketone molecules. Our electrochromic materials have several appealing properties, such as excellent colour intensity and contrasts, easy processability, a fast switching speed, and good durability and reversibility.

Results and discussion

Design and synthesis

The methyl ketone-bridged derivatives used in this study were prepared *via* the Friedel–Crafts acylation of aromatic rings with acid chlorides. In order to improve the acidity of the α-H and

[a]State Key Laboratory of Supramolecular Structure and Materials, College of Chemistry, Jilin University, Changchun, Jilin 130012, China. E-mail: liminjie@jlu.edu.cn; seanzhang@jlu.edu.cn; Fax: +86-431-85163812; Tel: +86-431-85163812

[b]Institute of Atomic and Molecular Physics, Jilin University, Changchun, Jilin 130012, China

† Electronic supplementary information (ESI) available: experimental procedures and synthesis. See DOI: 10.1039/c3tc30769g

facilitate the tautomerization, Ar1 was designed to include electron donating groups and Ar2 to include electron withdrawing groups. All of the compounds used in this paper were purified and fully characterized by conventional analytical methods, such as ^{1}H-NMR, ^{13}C-NMR, UV-Vis, MS *etc.* (Scheme 2 and ESI†).

Colour switching mechanism

Verification of the switch feasibility. As an example, the electro-switchable property of **M1** (Scheme 2) was first studied by cyclic voltammetry (CV) in acetonitrile (Fig. 1). A brilliant blue colour appeared when **M1** began to be reduced at −1.03 V, and disappeared at 0.2 V. The intensity of absorption was dependent on the redox state of **M1**, confirming that the colour switch can be triggered alternately by the electric field. What's more, the colour change was very obvious from colourless (λ_{max} = 273 nm) to bright blue (λ_{max} = 564 nm), with a maximum absorption wavelength red shift of 291 nm (Fig. 2).

Proof of the keto–enol tautomerization of M1. UV-Vis spectroscopy, IR, ^{1}H-NMR and GC (Gas Chromatography) spectroscopic analyses of both the electrically reduced and non-reduced **M1** solutions indicates the formation of the enolate isomer of **M1** during the electrical process. This conclusion is based on the fact that the absorption peak of the **M1** solution (564 nm, Fig. 2) after being electrically reduced is nearly identical to that of the enolate of **M1** (**M1-A**, 568 nm) generated by a strong chemical base (7 equivalents of *t*-BuOK in CH_3CN solution, Fig. 2). Additionally, its enolate structure is proved by ^{1}H-NMR spectroscopy (Fig. S2†). Furthermore, the IR data indicates clearly that the methyl ketone group is converted to the enolate (1548 cm^{-1}). Comparing the IR spectrum of the **M1** solution with its reduced solution at −1.2 V, a new peak representing C=C stretching absorption at 1548 cm^{-1} is observed, along with the decrease of the stretching vibration absorption intensities of both the carbonyl at 1687 cm^{-1} and the C–H of methylene at 1325 cm^{-1}.

In addition, the existence of the enolate **M1-A** in the electroreduction process is further proved by reaction with iodomethane. The blue colour of the reduced solution fades gradually after the addition of iodomethane, and **M8** is the only identified product obtained from the reaction. **M8** is confirmed to be a mono-methylated derivative of **M1** by ^{1}H-NMR and GC (Fig. S3 and S4†). This is further strong evidence proving the formation of **M1-A** during this electrochromic process.

The reduction process. To fully understand the electrochemical colour switching mechanism, detailed CV analyses of **M1** and its derivatives were performed. The reduction peak of

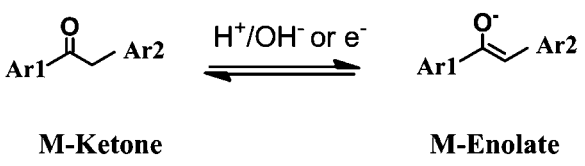

Scheme 1 Illustration of the design of the colour switches by bridging two aromatic motifs with a methyl ketone group.

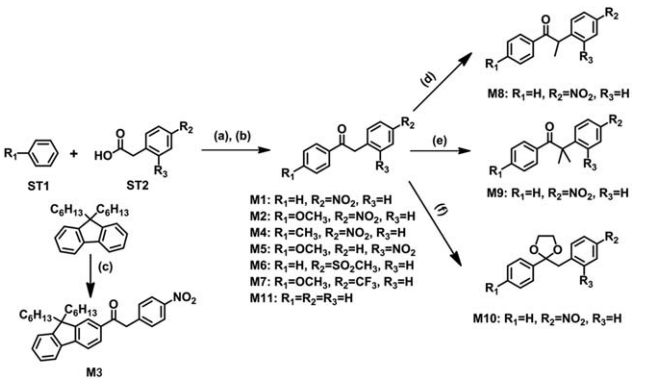

Scheme 2 Synthetic scheme for **M1–M11**. *Reagents*: (a) $SOCl_2$, CH_2Cl_2; (b) $AlCl_3$, CH_2Cl_2; (c) the same as (a) and (b) with different ST1; (d) $TBAPF_6$, CH_3I, CH_3CN, −1.2 V; (e) *t*-BuOK, CH_3I, THF, N_2; (f) ethylene glycol, *p*-toluene sulphonic acid, toluene.

M1 (−1.17 V) is assigned to the one-electron reduction of the nitro group rather than the carbonyl,[13] by comparison with those of nitrobenzene (−1.25 V) and **M11** (−2.0 V), a nitro-eliminated derivative of **M1**. The reduction of the nitro group is further confirmed by X-ray photoelectron spectroscopy (XPS) and infrared spectroscopy (IR). For **M1**, a single N 1s binding energy peak at 405.6 eV (Fig. 3A) for the nitro group is observed. However, when the **M1** solution is electrically reduced at −1.2 V, a new peak at 401.8 eV appears, which suggests that the nitro group is reduced under these conditions. In addition, a decrease in the nitro stretching absorptions (1517 cm^{-1}, 1352 cm^{-1}) of the blue reduced solution are observed, further indicating that the colour change is associated with the reduction of the nitro group (Fig. 3B).

However, no colour change is observed during the electrical reduction of the nitro group of **M9** (a two-substituted derivative on the methylene group of **M1**) and **M10** (a carbonyl-protected derivative of **M1**) (Fig. S1†). Those results clearly prove that the colour observed from the CV experiment of **M1** is closely related

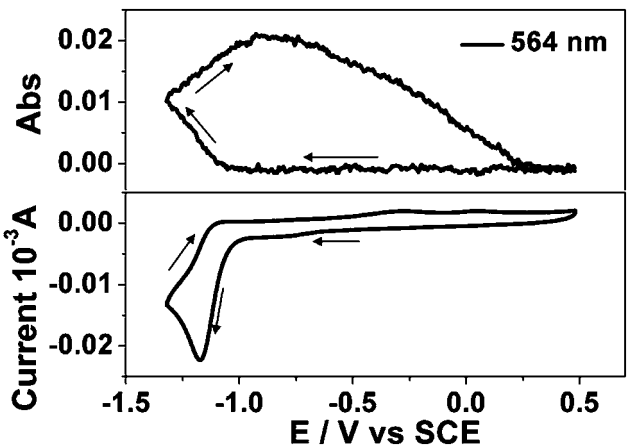

Fig. 1 (a) Changes in the absorption at 564 nm (top) and the cyclic voltammogram (bottom) of **M1** (1.0×10^{-3} M) in acetonitrile with 0.1 M $TBAPF_6$ using a glassy carbon electrode (d = 3 mm). Scan rate: 50 mV s^{-1}.

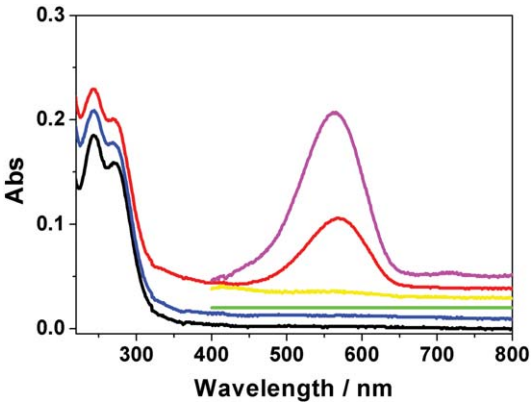

Fig. 2 Absorption spectra of **M1** (1.0×10^{-5} M) (black curve) in acetonitrile, treated with potassium *tert*-butoxide (red curve), and then neutralized with CH_3COOH (blue curve), and absorption spectra of **M1** (1.0×10^{-3} M) (green curve) in acetonitrile with 0.1 M $TBAPF_6$, stimulated by a −1.2 V voltage (pink curve), then by a 0.8 V voltage (yellow).

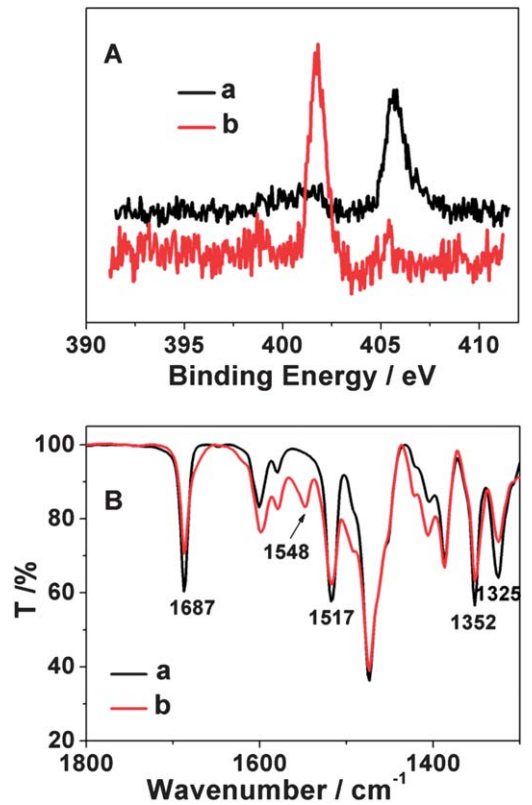

Fig. 3 (A) The XPS spectra of **M1** before (black curve) and after (red curve) reduction at −1.2 V in acetonitrile with 0.1 M $TBAPF_6$. (B) IR spectra of **M1** before (black curve) and after (red curve) reduction at −1.2 V in acetonitrile with 0.1 M $TBAPF_6$.

to the methyl ketone with an unsubstituted α-proton, which enables the molecules to undergo a keto–enol tautomerization.

Hypothesis of the mechanism. All of the results demonstrate that the electrically generated coloured intermediate is an enolate of the methyl ketone-bridged molecule (**M1-A**, an anion from the loss of a proton from **M1**) instead of a radical anion from the direct one-electron reduction of **M1**. Thus, we proposed that a radical anion (**M1-RA**, an "effective electro-base") is first generated from the one-electron reduction of the nitro group of **M1**. Then this "electro-base" produces the coloured **M1-A**, and turns itself into a radical (**M1-R**) by extracting a proton from nearby **M1** molecules. When **M1-R** loses a electron during the reverse process, a protonated cation (**M1-C**, an "effective electro-acid") is generated and reacts with a nearby **M1-A** molecule. Consequently, both species become the initial colourless ketone form.

The mechanism of the intermolecular proton transfer is supported by both theoretical and experimental evidence. The reversible colour change is observed when a mixture of nitrobenzene and the nitro-absent **M6** (or **M7**, Fig. S15 and S16†) is stimulated by an electric field. The observed colour is identical to the colour from **M6** (or **M7**) being treated with a chemical base. Meanwhile, any one of the species alone shows no colour change under the same treatment (Fig. S6 and 7†). In other words, even though **M6** and **M7** have no nitro group, their methyl ketone units can still be switched electrically in the presence of nitrobenzene under the reduction voltage of the nitro group *via* an intermolecular proton transfer between **M6** (or **M7**) and a radical anion of nitrobenzene.

The transformation from **M1** to **M1-RA** is exergonic by 6.4 kcal mol^{-1} (Fig. S17†), calculated with B3LYP/6-31+G(d,p),[14] which suggests that the reaction involving the intermolecular proton transfer is thermodynamically more favorable.

Thus, we could further conclude that the mechanism consists of the following processes. (i) **M1** is first converted to **M1-RA** through a one-electron reduction. Then the **M1-RA** ("electro-base") grabs a proton from the methylene group of a nearby **M1** molecule to generate **M1-R**[15] and **M1-A** (the colourant). (ii) When **M1-R** is transformed to the acidic **M1-C** *via* a one-electron oxidation, the **M1-C** gives the proton back to the **M1-A**. Then the protonated **M1-A** transforms back to **M1** again by the keto–enol tautomerization, and this process results in a colour reversal.

Performance of the colour switch

Response speed. The intermolecular proton transfer reaction induced by the radical anion ("electro-base") is very fast. There is still a change in colour even at a scan rate of 10 V s^{-1} in the CV experiment. Furthermore, a voltage impulse at 3.0 V for 50 ms can also result in a detectable colour change of the ITO devices (Fig. S10†). In addition, the colour intensity is found to increase gradually with the elevation of the voltage.

The stability and reversibility. To verify the stability and reversibility of the colour switch, the absorbance changes at 564 nm of **M1** in both a thin liquid film and a poly(methyl methacrylate) (PMMA) film in an ITO cell were monitored by UV-Vis spectroscopy (Fig. 5). The performance of 50 switching cycles for both the liquid and solid devices are shown in Fig. 5. For the solid device, there is much room to improve its stability and reversibility. These results confirm that this type of switchable molecule could be very stable under an inert environment, and **M1-A** and **M1-R** could be easily reversed back to the colourless **M1** without any observable side products.

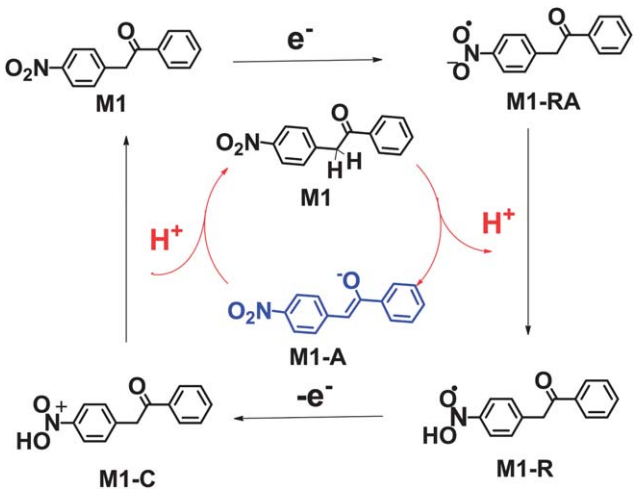

Fig. 4 The switch mechanism of **M1**.

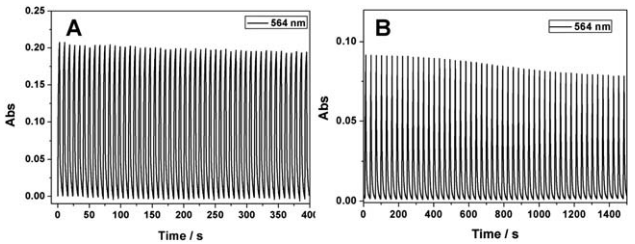

Fig. 5 (A) Absorbance variation (at 564 nm) of the thin liquid film of **M1** in an ITO device with the switch cycles generated by alternating −3.0 V (3 s) and 2.0 V (5 s) voltages. (B) Absorbance variation (at 564 nm) of the PMMA film of **M1** in an ITO device with the switch cycles generated by alternating −3.5 V (5 s) and 2.0 V (25 s) voltages.[16]

Colour tunability. Investigation into the colour tunability and switchability of **M1–M7** provides further insight into how substituent effects alter the electrochromic properties. Blue, yellow and green colours have been obtained by changing the conjugation length, as well as the electron-donating ability on the donor segments (Ar1) and electron-withdrawing ability on the acceptor segments (Ar2) (Fig. 6, Scheme 2). We find that increasing the conjugation length or adding a new donor group on the Ar1 side does not have a significant effect on the colour of the enolate isomers of **M1–M7**. This indicates that the oxygen anion portion of the coloured intermediates is a much stronger electron donor than Ar1, and it plays the dominant role in the colour. However, changing the electron-withdrawing functional group on Ar2 has pronounced effects on both the switchable colour and the switch threshold of the molecules. The *ortho*-positioned nitro group on Ar2 (**M5**) has a slightly higher switching potential value (from −1.03 V to −1.06 V) compared with its *para*-positioned counterpart in **M1**, but its maximum absorption is significantly red shifted from 564 nm to 601 nm. The CVs of **M1–M7** are shown in Fig. S11–S16.† The stronger the electron withdrawing nature of the acceptors, the lower the reduction potentials that are needed, and *vice versa*.

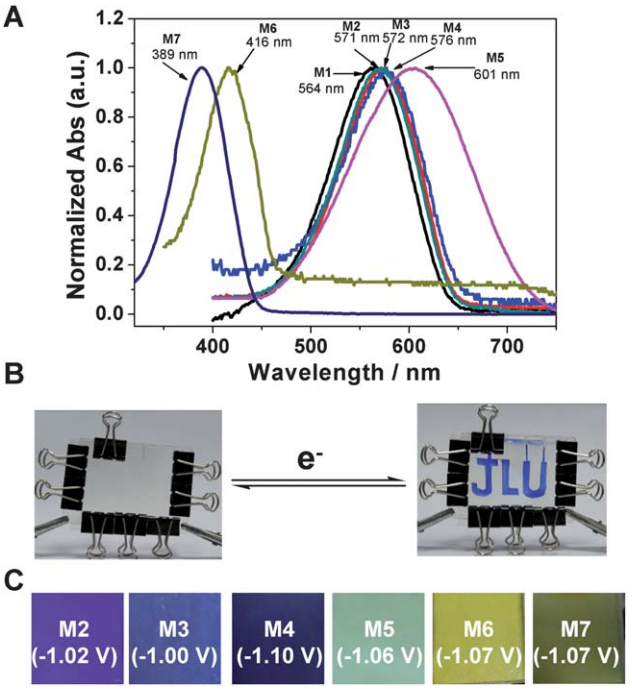

Fig. 6 (A) Absorption spectra of **M1–M7** in acetonitrile after the voltage is supplied. (B) A real object illustration of an electrically-driven display of "JLU" based on **M1**. (C) The real colour of **M2–M7** switched electrically in their ITO devices, with the switch threshold (from CV) provided in brackets (the switch thresholds of **M6** and **M7** are labelled as those of the mixture with nitrobenzene).

Conclusions

In conclusion, a new class of "electro-acid/base"-triggered reversible keto–enolate colour switches was proposed and demonstrated with methyl ketone-bridged molecules. The switching mechanism of intermolecular proton transfer induced by radical ions as an "electro-acid/base" has been clearly proved. The new colour switches are speedy and fairly durable, with several attractive properties such as large colour contrasts, colour tunability and good reversibility. A dramatic spectral absorption shift (of about 291 nm) is observed during the switching *via* keto–enolate tautomerization. Blue, yellow and green colours are obtained by adjusting either side of the substituents on the methyl ketone unit. The switching speed of the electrically-induced colour switching is less 50 ms. The colour switches are used in several prototype ITO devices, and repeated switching in the devices is achieved. This newly-demonstrated concept of "electro-acid/base" *in situ* for molecular switching is far more convenient than the conventional chemical stimulus of acids or bases for practical applications in IT devices, not only because the electric field is the simplest and easiest method for implementation, but also it can control both the reaction progress and direction quickly and precisely in a closed system based on the needs of the device. This important concept of using an "electro-acid/base" for the reversible manipulation of the molecular structure and properties will certainly inspire and accelerate the further development of broad switching materials and their applications in ultrathin flexible displays, data recording, sensing and optical communication, *etc.*

Experimental

Synthesis

The general synthetic procedure for **M1–M7** and **M11** using **M1** as a template is as follows: $SOCl_2$ (0.52 ml, 7.6 mmol, 1.2 eq.) was added to a solution of 2-(4-nitrophenyl)acetic acid (1.14 g, 6.3 mmol, 1 eq.) in dichloromethane (10 mL) at 25 °C and stirred for 4 h, then benzene (6 mmol, 1 eq.) and $AlCl_3$ (7.8 mmol, 1.3 eq.) were added in sequence to the above solution in an ice bath under a nitrogen atmosphere. After 4 h, the reaction mixture was poured onto ice, and the aqueous layer was extracted with ethyl acetate (3×10 mL). The combined organic layers were washed with brine and dried over $MgSO_4$. After being filtered and concentrated in vacuum, the product was separated by column chromatography using petroleum ether and ethyl acetate (v/v = 10 : 1) as the eluent.

Characterizations

The UV-Vis absorption spectra were measured using a Shimadzu UV-2550 PC double-beam spectrophotometer.

The cyclic voltammograms were obtained from a Bio-logic electrochemical work station. The experiments were performed under the protection of argon in acetonitrile containing $TBAPF_6$ (0.1 mol L^{-1}) as the supporting electrolyte. The three-electrode cell consisted of a glassy carbon working electrode (Shenhua, China) with a surface area of 7.07 mm^2, a Pt wire counter electrode (Shenhua, China) and an $AgNO_3$/Ag reference electrode (Shenhua, China). All of the redox potentials were referenced to internal ferrocene (E_0 (Fc^+/Fc^0) = 0.4 V *vs.* SCE), added at the end of each CV experiment.

The electron paramagnetic resonance (EPR) spectra were recorded on a JEOL JES-FA 200 EPR spectrometer.

The GC (Gas Chromatography) analysis was performed on a Shimadzu GCMS QP 2010 Plus instrument.

The ESI-HRMS analysis was performed on an Agilent 1290-micrOTOF-Q II mass spectrometer. Accurate masses were reported for the molecular ion $[M + H]^+$ or $[M]^+$.

The nuclear magnetic resonance spectra (^{1}H-NMR and ^{13}C-NMR) were recorded with a Varian Mercury (300 MHz). For $CDCl_3$ and CD_3CN solutions, the chemical shifts were reported as parts per million (ppm), referenced to the residual protium or carbon of the solvents; H in $CDCl_3$ (δ = 7.26 ppm) and C in $CDCl_3$ (δ = 77.0 ppm) or H in CD_3CN (δ = 1.94 ppm). The coupling constants are reported in Hertz (Hz).

The melting points were determined using a SGW X-4B microscopy melting point apparatus (Shanghai) and were uncorrected.

All of the calculations were performed using the Gaussian 09 program.[14] All of the molecules were fully optimized using the hybrid B3LYP functional with the 6-31G+(d,p) basis set. Then the vibrational spectrum of each molecule was calculated at the same level of theory to ensure that all of the structures correspond to the true minima of the potential energy surface.

Spectroelectrochemical characterizations

Changes in the solution absorption spectra were measured *in situ* during the potential sweep using a self-made spectroelectrochemical cell (shown in Fig. S18†). In order to measure the absorption spectra and the absorption lifetime of the ITO device under the *in situ* voltage application, the direct current mode was applied to the cell by a Bio-logic electrochemical work station.

Preparation of sandwich-type ITO cells

ITO cells sandwiched with liquid film. A two-electrode cell was constructed with ITO glass electrodes. The mixture solution containing methyl ketone-bridged molecules and $TBAPF_6$ was sandwiched between the ITO electrodes. Polydimethylsiloxane (PDMS) film was used as the spacer (shown in Fig. S19†).

ITO cells sandwiched with PMMA film. A mixture of 30 wt% of PMMA, 70 wt% of propylene carbonate, $TBAPF_6$ and the methyl ketone-bridged molecule was stirred for 24 h. A homogeneous phase with electrochromic properties was obtained. The above mixture film was laminated between two ITO electrodes. The thickness was set to about 0.1 mm (shown in Fig. S20†).

Acknowledgements

We thank Jilin University, State Key Lab of Supramolecular Structure and Materials for start-up support. This work was supported by the National Science Foundation of China (grant no. 21072025). The authors also acknowledge Prof. Erkang Wang, Dr Youxing Fang, Prof. Hansong Cheng, and Dr Shubin Zhao for helpful discussions relating to this project.

Notes and references

1 M. Berggren, D. Nilsson and N. D. Robinson, *Nat. Mater.*, 2007, **6**, 3; P. Beaujuge, S. Ellinger and J. Reynolds, *Nat. Mater.*, 2008, **7**, 795.
2 D. I. Gittins, D. Bethell, D. J. Schiffrin and R. J. Nichols, *Nature*, 2000, **408**, 67; C. Dri, M. V. Peters, J. Schwarz, S. Hecht and L. Grill, *Nat. Nanotechnol.*, 2008, **3**, 649; V. Ferri, M. Elbing, G. Pace, M. D. Dickey, M. Zharnikov, P. Samorì, M. Mayor and M. A. Rampi, *Angew. Chem., Int. Ed.*, 2008, **120**, 3455; S. J. van der Molen and P. Liljeroth, *J. Phys.: Condens. Matter*, 2010, **22**, 133001.
3 N. Shao, J. Jin, H. Wang, J. Zheng, R. Yang, W. Chan and Z. Abliz, *J. Am. Chem. Soc.*, 2009, **132**, 725; S. Zhu, M. Li, L. Sheng, P. Chen, Y. Zhang and S. X. Zhang, *Analyst*, 2012, **113**, 5581.
4 B. Champagne, A. Plaquet, J. L. Pozzo, V. Rodriguez and F. Castet, *J. Am. Chem. Soc.*, 2012, **134**, 8101; Y. Zhang, J. Martinez-Perdiguero, U. Baumeister, C. Walker, J. Etxebarria, M. Prehm, J. Ortega, C. Tschierske, M. J. O'Callaghan and A. Harant, *J. Am. Chem. Soc.*, 2009, **131**, 18386; Y. Matsuo, T. Ichiki and E. Nakamura, *J. Am. Chem. Soc.*, 2011, **133**, 9932.
5 P. Beaujuge and J. Reynolds, *Chem. Rev.*, 2010, **110**, 268.
6 J. Roncali, *Chem. Rev.*, 1992, **92**, 711; M. Mastragostino, C. Arbizzani, A. Bongini, G. Barbarella and M. Zambianchi, *Electrochim. Acta*, 1993, **38**, 135; M. Mastragostino,

C. Arbizzani, P. Ferloni and A. Marinangeli, *Solid State Ionics*, 1992, **53**, 471.

7 A. F. Diaz and J. A. Logan, *J. Electroanal. Chem.*, 1980, **111**, 111; A. Watanabe, K. Mori, Y. Iwasaki, Y. Nakamura and S. Niizuma, *Macromolecules*, 1987, **20**, 1793.

8 A. Patra and M. Bendikov, *J. Mater. Chem.*, 2010, **20**, 422; M. Li, A. Patra, Y. Sheynin and M. Bendikov, *Adv. Mater.*, 2009, **21**, 1707.

9 G. Chidichimo, D. Imbardelli, B. C. De Simone, P. Barone, M. Barberio, A. Bonanno, M. Camarca and A. Oliva, *J. Phys. Chem. C*, 2010, **114**, 16700; G. Chidichimo, M. De Benedittis, J. Lanzo, B. C. De Simone, D. Imbardelli, B. Gabriele, L. Veltri and G. Salerno, *Chem. Mater.*, 2007, **19**, 353; Y. Nishikitani, S. Uchida, T. Asano, M. Minami, S. Oshima, K. Ikai and T. Kubo, *J. Phys. Chem. C*, 2008, **112**, 4372.

10 W. Sharmoukh, K. C. Ko, J. H. Ko, H. J. Nam, D.-Y. Jung, C. Noh, J. Y. Lee and S. U. Son, *J. Mater. Chem.*, 2008, **18**, 4408; W. Sharmoukh, K. C. Ko, C. Noh, J. Y. Lee and S. U. Son, *J. Org. Chem.*, 2010, **75**, 6708; W. Sharmoukh, K. C. Ko, J. H. Ko, G. Jung, C. Noh, J. Y. Lee and S. U. Son, *Org. Lett.*, 2010, **12**, 3226.

11 L. Motiei, M. Lahav, D. Freeman and M. E. van der Boom, *J. Am. Chem. Soc.*, 2009, **131**, 3468.

12 P. Bednarek, Z. Zhu, T. Bally, T. Filipiak, A. Marcinek and J. Gebicki, *J. Am. Chem. Soc.*, 2001, **123**, 2377; R. R. Lozada-Garcia, J. Ceponkus, W. Chin, M. Chevalier and C. Crepin, *Chem. Phys. Lett.*, 2011, **504**, 142; X. Zhang, Z. Li, C. Lao, D. Zou, F. Lu, G. Lu, F. Du and F. Li, *Polymer*, 2006, **47**, 3390.

13 The reduction potential of the carbonyl group is about −2.0 V (*vs.* SCE), compared with **M6** (−2.0 V), **M7** (−2.1 V) and **M11** (−2.0 V), nitro-eliminated derivatives of **M1**.

14 M. J. Frisch, G. W. Trucks, H. B. Schlegel, G. E. Scuseria, M. A. Robb, J. R. Cheeseman, G. Scalmani, V. Barone, B. Mennucci, G. A. Petersson, H. Nakatsuji, M. Caricato, X. Li, H. P. Hratchian, A. F. Izmaylov, J. Bloino, G. Zheng, J. L. Sonnenberg, M. Hada, M. Ehara, K. Toyota, R. Fukuda, J. Hasegawa, M. Ishida, T. Nakajima, Y. Honda, O. Kitao, H. Nakai, T. Vreven, J. A. Montgomery, J. E. Peralta, F. Ogliaro, M. Bearpark, J. J. Heyd, E. Brothers, K. N. Kudin, V. N. Staroverov, R. Kobayashi, J. Normand, K. Raghavachari, A. Rendell, J. C. Burant, S. S. Iyengar, J. Tomasi, M. Cossi, N. Rega, J. M. Millam, M. Klene, J. E. Knox, J. B. Cross, V. Bakken, C. Adamo, J. Jaramillo, R. Gomperts, R. E. Stratmann, O. Yazyev, A. J. Austin, R. Cammi, C. Pomelli, J. W. Ochterski, R. L. Martin, K. Morokuma, V. G. Zakrzewski, G. A. Voth, P. Salvador, J. J. Dannenberg, S. Dapprich, A. D. Daniels, O. Farkas, J. B. Foresman, J. V. Ortiz, J. Cioslowski, and D. J. Fox, *Gaussian 09, (Revision A. 02)*, Gaussian, Inc., Wallingford, CT 2009.

15 The electron paramagnetic resonance (EPR) results (Fig. S5†) confirmed that a free radical was present in the blue solution.

16 The turn-on and turn-off voltages of the ITO device were determined by the CV performance of the solid and liquid devices, shown in Fig. S8 and S9†.

